Environmental Science & Technology

Article

pubs.acs.org/est

Hydrological Tracers Using Nanobiotechnology: Proof of Concept

Asha N. Sharma, Dan Luo, and M. Todd Walter*

Department of Biological and Environmental Engineering, Riley Robb Hall, Cornell University, Ithaca, New York 14853, United States

Supporting Information

ABSTRACT: In order to answer questions that involve differentiating among multiple and potentially interacting hydrological flowpaths, it would be ideal to use multiple tracers with identical transport properties that can nonetheless be distinguished from each other. This paper describes the development and proof of concept of a new kind of engineered tracer system that allows a large number of individual tracers to be simultaneously distinguished from one another. This new tracer is composed of polylactic acid (PLA) microspheres into which short strands of synthetic DNA and paramagnetic iron oxide nanoparticles are incorporated. The synthetic DNA serves as the "label" or "tag" in our tracers that allow us to distinguish one tracer from another, and paramagnetic iron oxide nanoparticles are included in the tracer to facilitate magnetic concentration of the tracers in potentially dilute water samples. Some potential advantages of this tracer concept include: virtually limitless uniquely labeled tracers, highly sensitive detection, and relatively moderate expense. Three proof-of-concept experiments at scales ranging from orders of 10 cm to 100 m demonstrated the use of the tracer system.

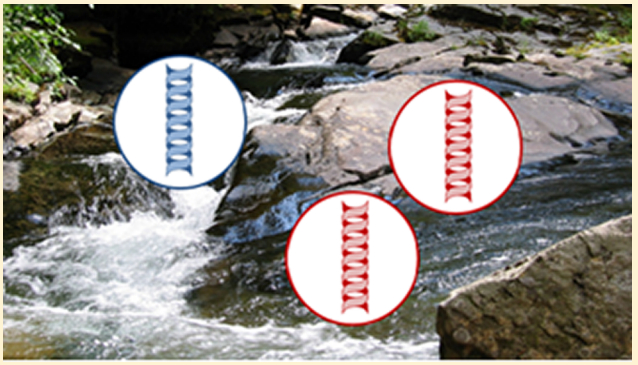

INTRODUCTION

Tracers are used extensively in hydrology to study flowpaths, flow velocities, hydrodynamic dispersion,[1] and other characteristics of water flow in the environment. Naturally occurring tracers such as chloride, silica, stable isotopes, and dissolved organic carbon have been used to identify contributions to streamwater from various "end-members"[2,3] and to distinguish among contributions attributed to different hydrological processes such as runoff,[4] shallow subsurface flow,[5] and deep groundwater.[6] Unfortunately, the ubiquity of these naturally occurring chemicals makes it difficult to identify a specific flowpath; i.e., even if such a tracer is associated with overland flow, it is rarely clear where the overland flow originated.[7]

To identify or characterize flowpaths more specifically, researchers often introduce tracers that can be detected above the natural background signals. A variety of traditional "artificial" or researcher-introduced tracers such as bromide,[8,9] chloride,[10,11] microspheres,[12] and dyes[1,13] have been used, but the applications of these are usually restricted to characterizing and/or visualizing known flowpaths at small spatial scales such as macropores,[14] plots,[10] hill slopes,[15] and stream reaches[11] because they become very dilute when applied to large scales such as watersheds. Moreover, watershed memory of past chemical inputs[16,17] and the sensitivity of streamwater chemical signals to interplay between biogeochemical and hydrological processes[18] further complicates the use of traditional tracers. There have been several studies that use microorganisms[19] and bacteriophages[20] as tracers; however, these involve limitations on size (which depends on the organism selected) and number of unique tracers with similar transport properties available. Hydrologists have also been resourceful about using "accidental" introductions of pollutant tracers (e.g., refs 21 and 22), but this approach is obviously not a reliable or versatile strategy.

In order to answer questions that involve multiple and potentially interacting hydrological flowpaths, multiple tracers with identical transport properties that can nonetheless be distinguished from each other are required. A powerful, direct application of such tracers would be the identification of potential sources of so-called nonpoint source pollution. There are only a few examples of such tracer systems in the literature including rare earth elements,[23,24] fluorobenzoic acid-based systems,[25−29] and DNA-based systems.[30,31] The fluorobenzoic acid-based system, while effective, has only a limited number (<10) of uniquely detectable tracers and is expensive.[27] Moreover, their retardation and degradation rates are not identical.[25,29] The rare earth element-based system is likewise hindered by a limited number of unique tracers, and the densities of the different tracers are both different from each other as well as much greater than that of water.[24] Thus, rare earth metals are really most appropriate when investigating surface water transport of sediments. For the DNA-based systems, there is essentially no limitation in number of unique

Received: April 20, 2012
Revised: July 20, 2012
Accepted: July 25, 2012
Published: July 25, 2012

tracers, nor substantial differences in retardation and degradation rates. Mahler et al.[30] attached synthetic DNA strands to silica and montmorillonite clay and measured the DNA concentration on the particles and in the supernatant over a three week period. No further studies were published with this system. Sabir et al.[31] evaluated a tracer composed of a synthetic DNA strand in a 12 m forced gradient steady-state field experiment for use in groundwater studies. Though the DNA moved somewhat differently than sodium chloride, the authors concluded that it could be useful as a groundwater tracer. Colleuille and Kitterod[32] used five naked-DNA (not attached to anything) tracers along with other methods to determine the potential source of a contamination incident in a municipal water well in Norway. It is not obvious why DNA-based tracers have not been used more; however, these previous studies do not protect the DNA and it is likely that the longevity of the tracers in the environment is short unless the DNA binds to clay or sand particles, humic substances,[33] or polycyclic aromatic hydrocarbons.[34]

We propose using nanobiotechnology to develop an engineered tracer system that allows a large number of individual tracers with essentially identical transport properties to be simultaneously distinguished from one another, has a low detection limit, is not prohibitively expensive, is environmentally safe, and for which we can control its degradation rate. This Article describes the development of the tracers, some proof-of-concept studies, and the next steps required to make this system reliable. Specifically, we demonstrate that the tracers are fabricated as we envision, test a system for concentrating the tracers, and run three small-scale, proof-of-concept experiments.

DNA-Based Tracer Concept. Our new tracer is composed of polylactic acid (PLA) microspheres into which short strands of synthetic DNA and paramagnetic iron oxide nanoparticles are incorporated. PLA is a polymer used here to bundle the DNA and magnetic nanoparticles into uniform and highly controllable nano- or micospheres. PLA is approved by the US Food and Drug Administration for medical applications and is commonly used in medical sutures and sustained release drug delivery systems.[35] Recently, it has also been used in compostable food containers. One attractive property of PLA is that it degrades over several weeks to months,[36] and the degradation time can be controlled by manipulating the composition of the polymer via additives.[37] Biodegradability is advantageous because it ensures that the tracers will neither pollute the environment nor hinder future experiments with its persistence, while also lasting long enough for the purposes of many hydrological investigations. We originally fabricated our tracers using medical-quality polymers but were able to reduce the cost by 4 orders of magnitude using the lower grade material used in compostable cups. The current cost is less than \$1 per gram of tracers (approximately 10^{12} individual tracers). The cost of analysis, primarily reagents and primers, is approximately \$2-\$3 per sample; this does not include labor. The cost of a qPCR instrument is comparable to an ion chromatograph, which is commonly used for analyzing ionic solute tracers. Access to qPCR facilities is becoming increasingly common, and the cost/96-well analyses at Cornell University is \$20−32[38] which is considerably less than \$1 per sample; the most expensive qPCR service we found was at the University of Colorado-Denver at \$126 per 96-well analysis,[39] which is still less than \$2 per sample.

The synthetic DNA serves as the "label" or "tag" in our tracers that allows us to distinguish one tracer from another. Strands of DNA (oligos) of 100 bases in length make their design and detection relatively simple and allow for an enormous number of unique tags; i.e., four different monomers in a strand of 100 results in $4^{100} = 1.61 \times 10^{60}$ unique sequences. Another advantage of DNA is that it allows us to use powerful biotechnology tools to "read" the tags, specifically, the polymerase chain reaction (PCR) and quantitative PCR (qPCR), which are highly sensitive methods for detecting DNA, even in very dilute quantities. PCR indicates the presence or absence of a specific DNA sequence, and qPCR allows us to quantify the number of specific DNA strands. Since the DNA strands are synthetic, that is, not derived from the genome of any organism, they do not have genetic functionality. There is sometimes public concern about introducing DNA into the environment, probably due to misconceptions about biotechnology in general. Sometimes, people fail to recognize that DNA is ubiquitous and we all introduce copious amounts of it into the environment every day. Even so, should concerns persist, we could use segments of uncommon DNA for our tags; for example, in the Northeastern US, we could develop tags based on palm DNA since palm trees are rare in that environment.

Paramagnetic iron oxide nanoparticles are included in the tracer to facilitate magnetic concentration of the tracers in water samples. This could be important when the tracers are applied to watershed-scale systems because we anticipate that the tracers will become very dilute. Paramagnetic iron oxide particles are being studied for a range of biomedical applications including contrast agents in MRI, in magnetic separation, in targeted drug delivery, and in treatment of tumors by hyperthermia.[40] Thus, we expect that there are low health risks in our application of this material. We recognize that there may be places that have naturally occurring magnetic materials in the soil or geology that could affect the movement of tracers infused with iron. In such situations, one would forego the inclusion of the iron oxide nanoparticles and consider using filtration to isolate the tracers from the water. These situations and alternative methods were outside the scope of this proof-of-concept project.

EXPERIMENTAL SECTION

Assessing Tracer Fabrication. The process for fabricating the tracers is described in the Supporting Information. The primary characteristics we needed to evaluate with respect to tracer fabrication were as follows: tracer size and uniformity, tracer detection and quantification, and magnetic concentration of tracers via the encapsulation of paramagnetic nanoparticles. Smith[41] and Smith et al.[42] measured many physical properties of PLA microspheres, including the zeta potential (−36.7 mV, standard deviation = 4.3 mV) and octanol−water partitioning coefficient (3.84, standard deviation = 0.68) [based on 1000 spheres, average diameter = 1 μm]. The degradation of PLA microspheres is complex but well understood (e.g., ref 43) and can be controlled by adding chemicals or changing the conditions (e.g., stirring time) during fabrication.[44−46] Smith et al.[42] characterized the stability of PLA microspheres by measuring the release of the material inside the spheres and found a rapid loss of about 30% of the material in the first few hours and then almost no additional loss for the next day. Luo et al.[35] found similar decay behavior and gradual degradation over several months. Other properties of the PLA microspheres

dx.doi.org/10.1021/es301561q | Environ. Sci. Technol. 2012, 46, 8928−8936

can be altered, e.g., size, surface charge, etc., and these are well described in the biomedical literature (e.g., refs 35, 45 and 47−49).

We used two approaches to assess tracer size and uniformity, scanning electron microscopy (SEM, Leica Stereoscan 440 Scanning Electron Microscope SEM) and dynamic light scattering (DLS, Brookhaven Instruments BI-200 SM Research Goniometer and Laser Light Scattering System). SEM analysis allowed us to visually verify that the microspheres were being successfully fabricated and assess their size. The tracers were mounted on an aluminum stub with double sided carbon tape. A Denton Vacuum Desk II sputter coater was used to coat the sample with a film of palladium/gold. The coated sample was observed under an accelerating voltage of 25 kV. DLS analysis was used to more generally determine the size distribution of the tracers. A small drop of 1 mg/mL sample was added to a sample vial filled with 12 mL of water.

We used qPCR to identify and quantify our tracers. To 150−200 μL of the tracer solution sample, an equal volume of chloroform was added to release the DNA from the PLA microsphere. The mixture was vortexed briefly and allowed to stand for 10 min. After 10 min of standing, the mixture was centrifuged. The aqueous supernatant which contained the DNA was removed using a micropipette and was stored at −20 °C until qPCR was performed. Quantitative PCR was performed on a Cepheid Smart Cycler II system using the Invitrogen SYBR GreenER qPCR Master Mix and a 25 μL total reaction volume per sample. Our detection limit was 100−1000 copies per 11 μL sample volume (see Supporting Information for standard curves); we are confident that this can be substantially reduced with more experience. Throughout this project, we assigned a value of zero to any samples below the detection limit. At the end of this project, we performed a BLAST analysis (see Supporting Information for details) to determine the likelihood of false positives due to environmental DNA that might, by chance, have similar sequences to our synthetic DNA-tags (see Supporting Information). Although we found relatively few similar sequences, in hindsight, we recommend that this analysis be done during the design of the DNA-tags to minimize the possibility of false positives.

To evaluate the efficacy of the use of paramagnetic nanoparticles in our tracer system, we first used transmission electron microscopy (TEM, FEI Tecnai T-12 Transmission Electron Microscope) to visually ascertain the incorporation of iron oxide nanoparticles into the tracers. A drop of 1 mg/mL tracer suspension was placed on a TEM grid and allowed to air-dry before observation.

To test the efficiency of the encapsulated paramagnetic nanoparticles, magnetic hysteresis curves of both pure iron oxide nanoparticles and iron oxide nanoparticles encapsulated in microspheres were measured using a vibrating sample magnetometer (VSM). Equal volumes of iron oxide suspension and acetone were taken in 1.5 mL microcentrifuge tubes. The samples were centrifuged at 8500 rpm for 10 min. The supernatant was discarded. The samples were dried at 45 °C for approximately 20 min in the Vacufuge (Eppendorf). Subsequently, 300 μL of acetone was added to each of the samples. They were centrifuged at 8500 rpm for 10 min, and the supernatant was discarded. The samples were dried at 30 °C for 15 min in the Vacufuge. Samples appeared to have white patches, presumably of oleic acid. Unlike the iron oxide nanoparticles, the tracer samples were not subject to any special treatment.

To more directly assess the magnetic separation or concentration component of our tracer system, a set of serial tracer suspensions ($1-10^{-5}$ g/L) was made and divided into two sets of 1.5 mL samples in 1.7 mL microcentrifuge tubes. One set of microcentrifuge tubes was placed against a magnet at a location where the magnetic field was at its maximum, and a second, control set was placed outside the magnetic field. The magnets used were rare earth Neodymium Boron magnets sealed in Stainless Steel (Eclipse Magnetics, SR240SHS) with a maximum field of ∼7600 G (measured by Alphalab, Inc. Model 1 gaussmeter) on the surface. These were kindly lent to us by Dr. Adrian Collins of ADAS, United Kingdom, Ltd. The tubes were left against the magnets overnight. For the tubes placed against the magnet, 1.4 mL of the "supernatant" was pipetted out, taking care to avoid touching the micropipette tip the wall of tube closest to the magnet. This was done so as to reduce disturbance to any aggregate of tracers that may have collected close to the magnet, i.e., to avoid remixing-up the dilute tracer solution. To the remaining water and tracers (the "concentrate") in the tube, 50 μL of water was added. Both the supernatant and concentrate samples analyzed using the qPCR. The control set, which was not in a magnetic field, was subject to the same procedure. For the control set, we were also careful to avoid pipetting from the bottom so that we did not accidentally resuspend tracers might have settled due to gravity.

Proof-of-Concept Transport Experiments. For our initial tracer experiments, we chose two simple systems to investigate the tracers' movement in porous media, that similar to soil or groundwater systems and a plot experiment to test the tracers' movement in overland flow. For our third proof-of-concept experiment, we applied the tracers to short stream reach. In these experiments, we use various combinations of three unique tracers, called Tracer 1, Tracer 2, and Tracer 3 for convenience.

Column Experiment. The primary objectives of this first, small-scale experiment were to confirm that the tracers would move through porous media and demonstrate that we could recover and quantify the tracers. A Chromaflex column from Kontes, 2.54 cm in diameter and 30.5 cm tall, was filled with quartz sand of grade 12/20 (Unimin Corporation) to a height of 24.5 cm. Water was pumped to the top of the column using a Masterflex Easy-Load II LS peristaltic pump from Cole Parmer (model 77200-50) with Masterflex 06419-13 (L/S-13) tygon tubing at a flow rate of 0.111 mL/s, which kept the column saturated for the duration of the experiment. The column was first adjusted to a steady-state flow of water and then switched to Tracer 2 suspension. The concentrations of tracer suspension used was 0.1 g/L. At 31.5 min, the input was switched back to water. Samples were collected at every 2−3 min, and subsequently, the DNA in them was quantified using the methods described above. A simple advection−dispersion model was applied to the experimental conditions to ascertain the degree to which the observed tracer breakthrough curves fit our theoretical understanding of how material moves through porous media.

Plot Experiment. The plot experiment was, among other things, carried-out at a much larger scale than the column experiment by approximately an order of magnitude relative to the column experiments (Figure 1). The primary objectives of this experiment were to test how similarly two uniquely labeled tracers moved (they should be essentially identical), confirm that we could distinguish two tracers from each other, and make sure we could detect and quantify the tracers when they

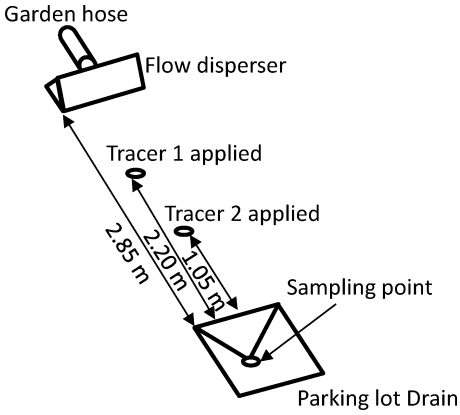

Figure 1. Plot experiment schematic. The tracers were applied simultaneously and instantaneously in a flow of velocity of 0.067 m/s.

were substantially more diluted than in the column experiment. We chose to run the experiments on an asphalt surface to avoid the complexities of soil and vegetation while maintaining some degree of nonidealized conditions. We also used this experiment to demonstrate the use of multiple (Tracers 1 and 2) tracers in a single experiment. Approximately 400 mg of tracers were dissolved in 200 mL of water. A steady stream with a velocity of 0.067 m/s was established. Tracers 1 and 2 were simultaneously and instantaneously introduced 1.05 and 2.2 m, respectively, from the sampling point, i.e., 1.8 and 0.65 m, respectively, from the source. Samples were nearly continuously collected in 100 mL sample bottles for 269 s; some water was lost between sample bottles. In order to reduce the number of samples for DNA quantification, only the even-numbered samples were analyzed. As with the column experiment, we applied a simple, one-dimensional advection−dispersion model with all parameters except dispersion independently measured. Because we presume that our tracers are identical with respect to transport characteristics, the only difference between the modeled pulses was the distance traveled.

Stream Experiment. The primary objectives of this experiment were to confirm that we could detect, quantify, and distinguish among the tracers in a much more diluting situation than either of the first two experiments and compare the transport of our tracers to a more conventional tracer, in this case, a dye. Two tracers (Tracers 2 and 3) were used in a small stream reach experiment near Ithaca, New York to increase the scale by approximately an order of magnitude over the plot experiment. The streamflow was 0.023 m^3/s. Approximately 1 g of Tracer 3 was introduced into the stream at the start of the experiment followed by approximately 1 g of Tracer 2 at the same point 300 s later. In order to visualize the flow, 50 mL of a blue food-grade dye (FD&C Blue No. 1, CAS No. 3844-45-9, Warner Jenkinson, concentration 13.4%) was added along with Tracer 3. Dyes are commonly used as tracers in hydrology (e.g., refs 50, 51, and 15, including for studies in rivers ref 50). Although this particular dye has been used widely to visualize preferential flow paths in vadose zone experiments,[52,53,13] it has been demonstrated that it is barely retarded even in sandy loams,[54] particularly at high flow rates.[55] Here, we use it in a surface flow setting at a high flow rate; thus, it can be expected to behave as a conservative tracer in this case. The dye's absorption spectrum is unaffected by ionic strength or pH.[56] Samples were collected in 100 mL plastic bottles simultaneously at four points, 6.1, 12.2, 36.6, and 61.0 m downstream of the point where the tracers were introduced, at times 10, 30, 60, 90, 120, 150, 180, 210, 240, 300, 360, 420, 480, 540, 600, 720 840, 960, 1080, and 1200 s after the start of the experiment. The samples were brought back to the lab and stored at ∼4 °C until analysis. The DNA in the samples was quantified using the procedure described earlier. The blue dye was quantified by measuring absorbance at 630 nm on a Milton Roy Spectronic 501 spectrophotometer.

RESULTS AND DISCUSSION

Assessing Tracer Fabrication. In the SEM observations, the microspheres appear smooth and a range of sizes were apparent, but most tracers appeared to be a few hundred nm across (Figure 2). The DLS measurements confirmed that the

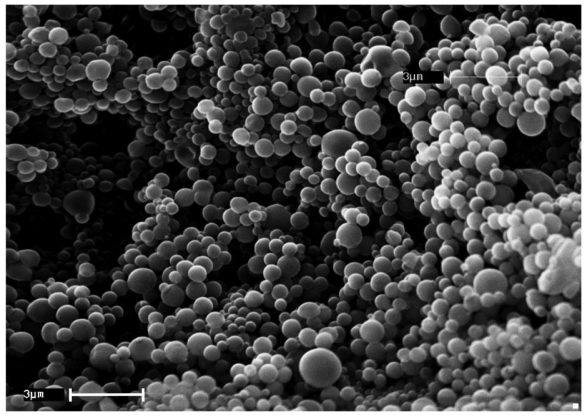

Figure 2. Representative SEM image of microspheres: the microspheres appear smooth and are mostly a few hundred nanometers in diameter.

mean microsphere size was measured around 400−500 nm (Figure 3). While a narrower size distribution may be desired for future experiments and may be obtained by other methods for making the microspheres, we saw no reason why this size distribution would be unsatisfactory for the preliminary experiments described here.

TEM images revealed evidence that the iron nanoparticles were successfully incorporated into the tracers, although we can

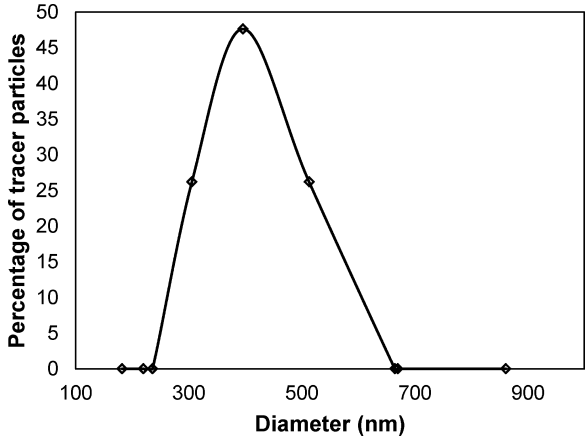

Figure 3. Distribution of microsphere size, as measured by DLS for one representative sample. The mean of the distribution is 454.8 nm. For the eight DLS measurements taken, the mean was 480.5 nm and the standard deviation was 59 nm.

dx.doi.org/10.1021/es301561q | *Environ. Sci. Technol.* 2012, 46, 8928−8936

only see them near the edges where there is sufficient transmission through the PLA (dark spots in Figure 4). The

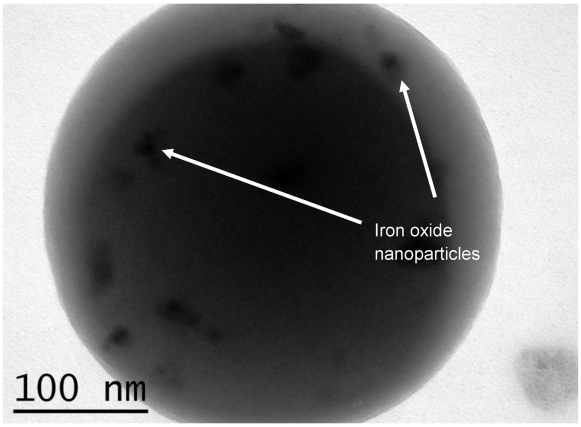

Figure 4. Representative TEM image of a microsphere: dark inclusions of iron oxide nanoparticles are seen.

VSM magnetic hysteresis curves confirmed that the microspheres are magnetized (Figure S2 in Supporting Information). As expected, the curves show that the microspheres have no magnetization when the magnetic field (**H**) is zero but are magnetized in the presence of an external magnetic field; this is the nature of paramagnetic materials. It is especially important that they have no magnetization in the absence of a magnetic field or they would potentially be attracted to naturally occurring iron in the environment. While the tracers containing iron oxide nanoparticles were clearly magnetized in the presence of a magnetic field, their strength was substantially lower than for the iron oxide nanoparticles alone, e.g., 2.6 vs 57 emu/g in a 15 kOe field (Figure S2 in Supporting Information). Iron oxide nanoparticles are often coated with surfactants or other materials to protect them from aggregation and oxidation.[57] In this case, oleic acid serves this function.[58]

In the magnetic separation experiments, aggregates of tracers could be visually observed near the magnet, further verifying the incorporation of the iron oxide nanoparticles in the tracers. Magnetic separation concentrated the microspheres 5- to 15-fold, depending on the original concentration (Table 1). In contrast, separation by gravitational settling in the control set for the same period of time concentrated the microspheres up to 4-fold (Table 1). We generally observed increasing relative concentration for the magnetic separation except at the highest concentrations where we speculate aggregated tracers interfered with the reach of the magnetic field, i.e., the depth of build-up of tracers near the magnet in essence blocked tracers further from the magnet. The magnetic separation setup used here is rudimentary and meant to qualitatively show the potential for this method. The consistently better performance of magnetic separation relative to the controls both in terms of actual concentration (as measured by qPCR) as well as visual verification of separation supports the view that magnetic separation may be a promising approach for concentrating dilute tracer samples where large sample volumes may make concentration by filtration difficult. Before magnetic separation can be used in this setting, further work is needed in developing a consistent magnetic separation method and determining the efficiency of magnetic separation at various concentrations. Note: we had no detection problems in our proof-of-concept experiments that required further development of the magnetic separation method.

Table 1. Results of Magnetic Separation Experiment[a]

original concentration (g/L)	relative concentrate (magnetic separation)/ original	relative concentrate (gravity separation)/ original
1	5.8	3.4
10^{-1}	5.8	2.9
10^{-2}	10.6	2.2
10^{-3}	15.0	4.5
10^{-4}	7.4	1.2
10^{-5}	7.2	2.5

[a]The second and third columns refer to concentration of DNA in the concentrate obtained by magnetic separation and gravity separation, respectively, versus that in the original suspension.

Proof-of-Concept Experiments. *Column Experiment.* The tracer data agreed relatively well with a simple one-dimensional advection–dispersion model[59] with a dispersion coefficient (D) of 1404 m^2/s, although there was more scatter in the data than desired (Figure 5). We do not yet know if the

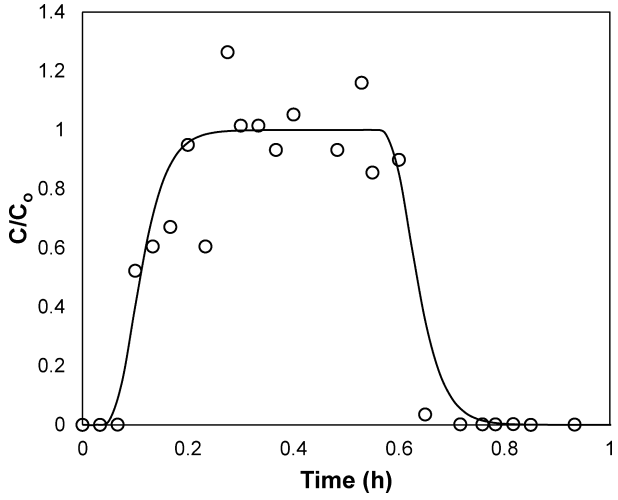

Figure 5. Breakthrough curve for column experiment. The circles are data; the line represents a simple advection dispersion model for the same system, with a dispersion coefficient of 0.039 m^2/h.

transport mechanisms implicit in this model are directly applicable to our tracers, but this model is often calibrated to capture the temporal patterns of environmental transport, even when the actual transport mechanisms would seem to make the model inappropriate (e.g., ref 60). In the case of this sand column, the tracers moved at the same speed as the water; i.e., the advection term that resulted in the best-fit of the model to the tracers was equal to the velocity of the water. However, we anticipate that the tracers will move somewhat faster than the bulk water in an undisturbed soil with macropores.[61,62] The next step is to use an undisturbed soil column to see the degree to which the tracers favor preferential flow paths. For this proof-of-concept, however, we only wanted to demonstrate that the tracers would move through porous media in a reasonably well-behaved fashion. We speculate that the substantial scatter in our data can be reduced as we improve our qPCR technique, particularly our design of oligos and primers. However, it is likely that the observed scatter in our data was inherent to our experimental setup; for example, the peristaltic pump may have

dx.doi.org/10.1021/es301561q | Environ. Sci. Technol. 2012, 46, 8928–8936

added tracers as a series of pulses that did not entirely disperse over such a small distance while moving through the sand column. A previous study found that PLA microspheres will attach and detach from the sand particles,[42] which may explain some of the scatter. However, the previous study also found that the "stickiness" of the PLA microspheres retarded the breakthrough and we did not observe that here. Further research is needed to better understand the interactions between the tracers and porous media.

Plot Experiment. The tracer data also agreed reasonably well with a simple one-dimensional advection–dispersion (D = 0.005 m^2/s) model for the plot experiment (Figure 6). As with the column experiment, the use of this model was to assess bulk behavior of the tracers rather than to assess specific transport processes. For example, as with the column experiment, we found that the tracers' speed was equal to that of the water. The model also indicated that there was an unanticipated, large loss of tracers, at about 85% loss. This loss was not a continuous sink because both tracers lost the same amount of material. If it was some sort of continuous loss, we would expect more loss for Tracer 1 because it was located further from the collection point, i.e., we would have needed a continuous loss-term in the model to fit it to the tracer data. We speculate that, in order to ensure detection, we applied too many tracers at each point, which lead to unintended aggregation and settling of some of the tracers. The difference between peak concentrations (Figure 6) is entirely due to dispersion. Except for the initial loss of tracers, they were relatively well behaved and exhibited much less variability than was seen in the small scale experiment, which supports our speculation that some of the variability observed in the column experiment was due to the small scale and inherent variability in flow. For the plot experiment, the deviation in the tail between the data and model, especially for Tracer 2 (Figure 6), is consistent with recent research on wash-off from hard urban surfaces, including both idealized[63,64] and "natural" urban surfaces.[65] In short, this experiment confirmed that we can fabricate uniquely distinguishable tracers with essentially identical transport characteristics in overland flow.

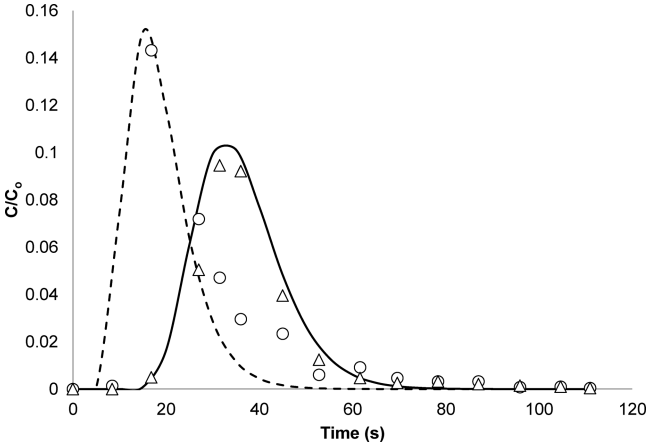

Figure 6. Result of plot experiment. Circles are Tracer 1 data; triangles are Tracer 2 data; the dashed line represents the model for Tracer 1; the continuous line represents the same model for Tracer 2.

Stream Experiment. The Tracer 3 and blue dye, which were introduced into the flow simultaneously, followed a similar pattern in time, with the peaks matching at all the locations with the possible exception that Tracer 3 peaked slightly before the dye at 61 m. This indicates that in this larger system, relative to the column and plot experiments, the tracer moves similarly to a dye. Interestingly, the tracer recoveries were about twice as efficient as the dye, perhaps because the dye might have been adsorbed on the stream bed material and vegetation. The peaks for Tracer 2 are not as well captured as for Tracer 3 because the sampling interval after Tracer 2 was introduced was much larger; note that Tracer 3 peaked at 6.1 m downstream in 30 s, and 60 s had elapsed before our first sampling after Tracer 2 was introduced. Thus, we would not expect to capture this peak; the peaks at 36.6 and 61.0 m were similarly missed because the interval between sampling was even longer at the times we would expect to have seen Tracer 2 at those locations. However, Tracer 3 peaked 12.2 m downstream in 60 s which matches the arrival time for Tracer 2 to peak at the same location (Figure 7B). We are not sure why the Tracer 2 peak is so high at this point. This experiment also demonstrates that

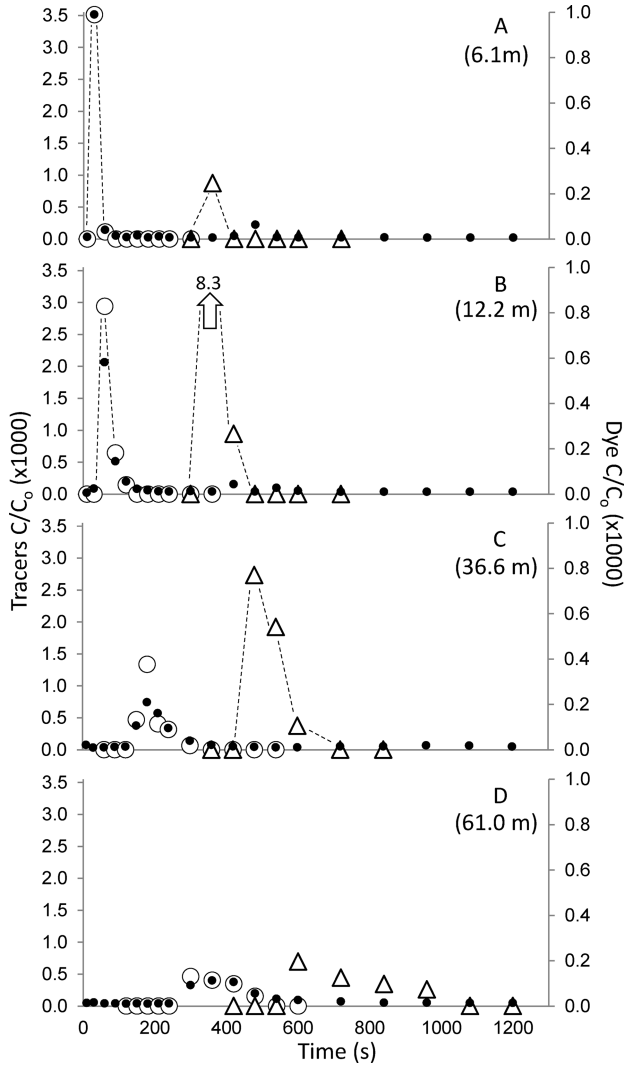

Figure 7. C/C_o denotes measured concentration over initial concentration (concentration of introduced tracer or dye). A, B, C, and D indicate the sampling points at increasing distance (6.1, 12.2, 36.6, and 61.0 m) downstream from the introduction point. Open circles = Tracer 3, open triangles = Tracer 2, and solid circles = blue dye. The arrow in "B" indicates that Tracer 2 C/C_o was 8.3×10^{-3}, which is above the bounds of the vertical axis shown.

dx.doi.org/10.1021/es301561q | Environ. Sci. Technol. 2012, 46, 8928–8936

the tracers transport properties are essentially identical at this larger scale, with timing of the peaks matching. The concentrations between the tracers do not match, possibly because the periodic sampling strategy resulted in missing peaks for one tracer or the other.

CONCLUSIONS AND NEXT STEPS

These preliminary experiments show encouraging potential for this new tracer system. In this proof-of-concept, we were unable to explore many of the potential opportunities our new tracers offer because many of their properties can be altered. For example, one could fabricate tracers that are essentially identical in every way except one, e.g., zeta potential, for which the effects on colloid transport require further investigation.[66] We are currently working on ways to speed-up the production of the tracers, which is currently the bottleneck of our proposed system and requires substantial labor. Luckily, the process is simple enough that we were able to train five undergraduate research assistants to fabricate the tracers, which was much more cost-effective than using graduate students, postdocs, and staff. We are also investigating alternative methods for more reliably and easily quantifying tracers in collected samples. One approach that appears to be especially promising is the use of DNA-based fluorescent nanobarcodes (e.g. 67 and 68), which can be "read" (multiplexed) with inexpensive portable microchips currently under development in Cornell's Luo Lab (Dr. Dan Luo, personal communication). We are also exploring additional magnetic concentration systems in which the sample is poured through (in the lab) or flows through (in the field) magnetized material upon which the tracers would accumulate. The next field demonstration steps are: (1) to run plot scale storm runoff experiments under rainfall conditions on both impermeable (asphalt) and permeable (soil) surfaces, (2) a small watershed (10 ha) experiment, which is instrumented and ready for use in fall 2012, and (3) groundwater experiments for which a research proposal has been submitted.

ASSOCIATED CONTENT

Supporting Information

Fabricating tracers, BLAST analysis, standard curves for qPCR, and hysteresis curves from vibrating sample magnetometer (VSM) analysis. This material is available free of charge via the Internet at http://pubs.acs.org.

AUTHOR INFORMATION

Corresponding Author

*E-mail: mtw5@cornell.edu; phone: 607-255-2488; fax: 607-255-2488.

Notes

The authors declare no competing financial interest.

ACKNOWLEDGMENTS

Funding for this research was granted by the NSF-CBET (Award # 0853809) and the USDA-NRI CGP Nanoscale Science and Engineering for Agricultural and Food Systems program (Title: Using nanotechnology to identify and characterize hydrological flowpaths in agricultural landscapes). This work made use of the SEM, TEM, and DLS facilities of the Cornell Center for Materials Research (CCMR) with support from the National Science Foundation Materials Research Science and Engineering Centers (MRSEC) program (DMR 1120296). We would also like to thank Dr. John Regan of Pennsylvania State University for his qPCR help; John Hunt and Yuanming Zhang of the Cornell Center for Materials Research for help with SEM, TEM, and DLS; and the following Cornell students for assistance with fabricating tracers and running experiments: Brian Buchanan, Meghan Fitzgerald, Ry Forseth, Daniel R. Fuka, Rebecca (Becky) Marjerison, Lauren McPhillips, Rustom Meyer, Vania Pereira, Rachel Perlman, Jonathan Petrie, Erik Rassmussen, Angela Rigden, Stephen Shaw, Emily Stockwell, and Thua Tran. We would also like to acknowledge the early PLA-tracer work by Jennifer Smith.[41,42] Finally, we thank the associate editor and four anonymous reviewers for the suggestions to improve this manuscript.

REFERENCES

(1) Flury, M.; Wai, N. N. Dyes as tracers for vadose zone hydrology. *Rev. Geophys.* **2003**, *41*, 1002−1038.

(2) Hooper, R. P.; Christophersen, N.; Peters, N. E. Modeling streamwater chemistry as a mixture of soilwater end-members: An application to the Panola Mountain Catchment, Georgia, USA. *J. Hydrol.* **1990**, *116*, 321−343.

(3) Christophersen, N.; Hooper, R. P. Multivariate-analysis of stream water chemical-data: The use of principal components-analysis for the end-member mixing problem. *Water Resour. Res.* **1992**, *28*, 99−107.

(4) Burns, D. A.; Kendall, C. Analysis of $\delta^{15}N$ and $\delta^{18}O$ to differentiate NO_3^- : Sources in runoff at two watersheds in the Catskill Mountains of New York. *Water Resour. Res.* **2002**, *38*, 1051−1061.

(5) Brown, V. A.; McDonnell, J. J.; Burns, D. A.; Kendall, C. The role of event water, a rapid shallow flow component, and catchment size in summer stormflow. *J. Hydrol.* **1999**, *217*, 171−190.

(6) McGuire, K. J.; DeWalle, D. R.; Gburek, W. J. Evaluation of mean residence time in subsurface waters using oxygen-18 fluctuations during drought conditions in the mid-Appalachians. *J. Hydrol.* **2002**, *261*, 132−149.

(7) Pfister, L.; McDonnell, J. J.; Wrede, S.; Hlubikova, D.; Matgen, P.; Fenicia, F.; Ector, L.; Hoffmann, L. The rivers are alive: On the potential for diatoms as a tracer of water source and hydrological connectivity. *Hydrol. Process.* **2009**, *23*, 2841−2845.

(8) Knopman, D. S.; Voss, C. I.; Garabedian, S. P. Sampling design for groundwater solute transport: Tests of methods and analysis of Cape-Cod tracer test data. *Water Resour. Res.* **1991**, *27*, 925−949.

(9) Jorgensen, P. R.; Helstrup, T.; Urup, J.; Seifert, D. Modeling of non-reactive solute transport in fractured clayey till during variable flow rate and time. *J. Contam. Hydrol.* **2004**, *68*, 193−216.

(10) Dyck, M. F.; Kachanoski, R. G.; de Jong, E. Long-term movement of a chloride tracer under transient, semi-arid conditions. *Soil Sci. Soc. Am. J.* **2003**, *67*, 471−477.

(11) Lautz, L. K.; Siegel, D. I.; Bauer, R. L. Impact of debris dams on hyporheic interaction along a semi-arid stream. *Hydrol. Process.* **2006**, *20*, 183−196.

(12) Metge, D. W.; Harvey, R. W.; Anders, R.; Rosenberry, D. O.; Seymour, D.; Jasperse, J. Use of carboxylated microspheres to assess transport potential of *Cryptosporidium parvum* oocysts at the Russian River water supply facility, Sonoma County, California. *Geomicrobiol. J.* **2007**, *24*, 231−245.

(13) Heilig, A.; Steenhuis, T. S.; Walter, M. T.; Herbert, S. J. Funneled flow mechanisms in layered soil: Field investigations. *J. Hydrol.* **2003**, *279*, 210−223.

(14) Bouma, J.; Jongerius, A.; Boersma, O.; Jager, A.; Schoonderbeek, D. Function of different types of macropores during saturated flow through 4 swelling soil horizons. *Soil Sci. Soc. Am. J.* **1977**, *41*, 945−950.

(15) McGuire, K. J.; Weiler, M.; McDonnell, J. J. Integrating tracer experiments with modeling to assess runoff processes and water transit times. *Adv. Water Resour.* **2007**, *30*, 824−837.

(16) Scott, C. A.; Walter, M. F.; Nagle, G. N.; Walter, M. T.; Sierra, N. V.; Brooks, E. S. Residual phosphorus in runoff from successional forest on abandoned agricultural land: 1. Biogeochemical and hydrological processes. *Biogeochemistry* **2001**, *55*, 293−309.

(17) Kirchner, J. W.; Feng, X. H.; Neal, C. Fractal stream chemistry and its implications for contaminant transport in catchments. *Nature* **2000**, *403*, 524−527.
(18) Hornberger, G. M.; Scanlon, T. M.; Raffensperger, J. P. Modelling transport of dissolved silica in a forested headwater catchment: The effect of hydrological and chemical time scales on hysteresis in the concentration-discharge relationship. *Hydrol. Process.* **2001**, *15*, 2029−2038.
(19) Harvey, R. W. Microorganisms as tracers in groundwater injection and recovery experiments: A review. *FEMS Microbiol. Rev.* **1997**, *20*, 461−472.
(20) Rossi, P.; Dorfliger, N.; Kennedy, K.; Muller, I.; Aragno, M. Bacteriophages as surface and ground water tracers. *Hydrol. Earth Syst. Sci.* **1998**, *2*, 101−110.
(21) Ekwurzel, B.; Schlosser, P.; Smethie, W. M.; Plummer, L. N.; Busenberg, E.; Michel, R. L.; Weppernig, R.; Stute, M. Dating of shallow groundwater: Comparison of the transient tracers H-3/H-E-3 chlorofluorocarbons, and Kr-85. *Water Resour. Res.* **1994**, *30*, 1693−1708.
(22) Rademacher, L. K.; Clark, J. F.; Boles, J. R. Groundwater residence times and flow paths in fractured rock determined using environmental tracers in the mission tunnel; Santa Barbara County, California, USA. *Environ. Geol.* **2003**, *43*, 557−567.
(23) Matisoff, G.; Ketterer, M. E.; Wilson, C. G.; Layman, R.; Whiting, P. J. Transport of rare earth element-tagged soil particles in response to thunderstorm runoff. *Environ. Sci. Technol.* **2001**, *35*, 3356−3362.
(24) Zhang, X. C.; Friedrich, J. M.; Nearing, M. A.; Norton, L. D. Potential use of rare earth oxides as tracers for soil erosion and aggregation studies. *Soil Sci. Soc. Am. J.* **2001**, *65*, 1508−1515.
(25) Bowman, R. S.; Gibbens, J. F. Difluorobenzoates as nonreactive tracers in soil and ground-water. *Ground Water* **1992**, *30*, 8−14.
(26) Benson, C. F.; Bowman, R. S. Tri-fluorobenzoates and tetrafluorobenzoates as nonreactive tracers in soil and groundwater. *Soil Sci. Soc. Am. J.* **1994**, *58*, 1123−1129.
(27) Kung, K. J. S.; Kladivko, E. J.; Gish, T. J.; Steenhuis, T. S.; Bubenzer, G.; Helling, C. S. Quantifying preferential flow by breakthrough of sequentially applied tracers: Silt loam soil. *Soil Sci. Soc. Am. J.* **2000**, *64*, 1296−1304.
(28) Dahan, O.; Nativ, R.; Adar, E. M.; Berkowitz, B.; Ronen, Z. Field observation of flow in a fracture intersecting unsaturated chalk. *Water Resour. Res.* **1999**, *35*, 3315−3326.
(29) Jaynes, D. B. Evaluation of fluorobenzoate tracers in surface soils. *Ground Water* **1994**, *32*, 532−538.
(30) Mahler, B. J.; Winkler, M.; Bennett, P.; Hillis, D. M. DNA-labeled clay: A sensitive new method for tracing particle transport. *Geology* **1998**, *26*, 831−834.
(31) Sabir, I. H.; Torgersen, J.; Haldorsen, S.; Alestrom, P. DNA tracers with information capacity and high detection sensitivity tested in groundwater studies. *Hydrogeol. J.* **1999**, *7*, 264−272.
(32) Colleuille, H.; Kitterod, N. O. *Forurensning av drikkevannsbronn pa Sundreoya i Al kommune: Resultat av sporstoff-forsok*; Norwegian Water Resources and Energy Directorate Report; Oslo, June **1998**; in Norwegian.
(33) Pietramellara, G.; Ascher, J.; Borgogni, F.; Ceccherini, M. T.; Guerri, G.; Nannipieri, P. Extracellular DNA in soil and sediment: Fate and ecological relevance. *Biol. Fertil. Soils* **2009**, *45*, 219−235.
(34) Kang, F. X.; Gao, Y. Z.; Wang, Q. A. Inhibition of free DNA degradation by the deformation of DNA exposed to trace polycyclic aromatic hydrocarbon contaminants. *Environ. Sci. Technol.* **2010**, *44*, 8891−8896.
(35) Luo, D.; Woodrow-Mumford, K.; Belcheva, N.; Saltzman, W. M. Controlled DNA delivery systems. *Pharm. Res.* **1999**, *16*, 1300−1308.
(36) Beck, L. R.; Cowsar, D. R.; Lewis, D. H.; Gibson, J. W.; Flowers, C. E. New long-acting injectable microcapsule contraceptive system. *Obstet. Gynecol.* **1979**, *135*, 419−426.
(37) Anderson, J. M.; Shive, M. S. Biodegradation and biocompatibility of PLA and PLGA microspheres. *Adv. Drug Delivery Rev.* **1997**, *28*, 5−24.
(38) Cornell University Life Sciences Core Laboratories Center Price Schedule (Genomics). http://www.brc.cornell.edu/brcinfo/?p=price&f=1 (accessed July 12, 2012).
(39) The Regents of the University of Colorado PCR Service. http://www.ucdenver.edu/academics/colleges/medicalschool/centers/cancercenter/Research/sharedresources/genomics/Pages/PCR.aspx (accessed July 18, 2012).
(40) Pankhurst, Q. A.; Connolly, J.; Jones, S. K.; Dobson, J. Applications of magnetic nanoparticles in biomedicine. *J. Phys. D: Appl. Phys.* **2003**, *36*, R167−R181.
(41) Smith, J. *Colloid Transport in Porous Media: Modeling Column Scale Transport with Rate Constants Calculated from Pore Scale Observations*; Cornell University: Ithaca, NY, August **2006**.
(42) Smith, J.; Gao, B.; Funabashi, H.; Tran, T. N.; Luo, D.; Ahner, B. A.; Steenhuis, T. S.; Hay, A. G.; Walter, M. T. Pore-scale quantification of colloid transport in saturated porous media.*Environ. Sci. Technol.* **2008**, *42*, 517−523.
(43) Batycky, R. P.; Hanes, J; Langer, R; Edwards, D. A. A theoretical model of erosion and macromolecular drug release from biodegrading microspheres. *J. Pharm. Sci.* **1997**, *86*, 1464−1477.
(44) Cleland, J. L.; Jones, A. J. Stable formulations of recombinant human growth hormone and interferon-gamma for microencapsulation in biodegradable microspheres. *Pharm. Res.* **1996**, *13*, 1464−1475.
(45) Luo, D.; Woodrow-Mumford, K.; Belcheva, N.; Saltzman, W. M. DNA controlled release systems using implantable matrices and injectable microspheres. *Proc. Int. Symp. Control. Rel. Bioact. Mater.* **1999**, 1098−1099.
(46) Luo, D.; Saltzman, W. M. Synthetic DNA delivery systems. *Nat. Biotechnol.* **2000**, *18*, 33−37.
(47) Mahoney, M. J.; Saltzman, W. M. Controlled release of proteins to tissue transplants for the treatment of neurodegenerative disorders. *J. Pharm. Sci.* **1996**, *85*, 1276−1281.
(48) Krewson, C. E.; Dause, R.; Mak, M.; Saltzman, W. M. Stabilization of nerve growth factor in controlled release polymers and in tissue. *J. Biomater. Sci., Polym. Ed.* **1996**, *8*, 103−117.
(49) Fung, L. K.; Saltzman, W. M. Polymeric implants for cancer chemotherapy. *Adv. Drug Delivery Rev.* **1997**, *26*, 209.
(50) Kratzer, C. R.; Biagtan, R. N. *Determination of Traveltimes in the Lower San Joaquin River Basin, California, from Dye-Tracer Studies during 1994−1995*; U. S. Geological Survey, National Water-Quality Assessment Program; Branch of Information Services, U.S. Geological Survey, U.S. Dept. of the Interior: Sacramento, Calif.; Denver, CO, 1997.
(51) Fernald, A. G.; Wigington, P. J.; Landers, D. H. Transient storage and hyporheic flow along the Willamette River, Oregon: Field measurements and model estimates. *Water Resour. Res.* **2001**, *37*, 1681−1694.
(52) Akhtar, M. S.; Richards, B. K.; Medrano, P. A.; DeGroot, M.; Steenhuis, T. S. Dissolved phosphorus from undisturbed soil cores: Related to adsorption strength, flow rate, or soil structure? *Soil Sci. Soc. Am. J.* **2003**, *67*, 458−470.
(53) Walter, M. T.; Kim, J. S.; Steenhuis, T. S.; Parlange, J. Y.; Heilig, A.; Braddock, R. D.; Selker, J. S.; Boll, J. Funneled flow mechanisms in a sloping layered soil: Laboratory investigation. *Water Resour. Res.* **2000**, *36*, 841−849.
(54) Flury, M.; Fluehler, H. Tracer characteristics of Brilliant Blue FCF. *Soil Sci. Soc. Am. J.* **1995**, *59*, 22−27.
(55) Perillo, C. A.; Gupta, S. C.; Nater, E. A.; Moncrief, J. F. Flow velocity effects on the retardation of FD&C Blue no. 1 food dye in, soil. *Soil Sci. Soc. Am. J.* **1998**, *62*, 39−45.
(56) German-Heins, J.; Flury, M. Sorption of Brilliant Blue FCF in soils as affected by pH and ionic strength. *Geoderma* **2000**, *97*, 87−101.
(57) Jiang, W.; Lai, K.; Hu, H.; Zeng, X.; Lan, F.; Liu, K.; Wu, Y.; Gu, Z. The effect of $[Fe^{3+}]/[Fe^{2+}]$ molar ratio and iron salts concentration on the properties of superparamagnetic iron oxide nanoparticles in the water/ethanol/toluene system. *J. Nanopart. Res.* **2011**, *13*, 5135−5145.
(58) Liu, X.; Kaminski, M. D.; Guan, Y.; Chen, H.; Liu, H.; Rosengart, A. J. Preparation and characterization of hydrophobic

superparamagnetic magnetite gel. *J. Magn. Magn. Mater.* **2006**, *306*, 248−253.
(59) Freeze, R. A.; Cherry, J. A. *Groundwater*; Prentice-Hall: Englewood Cliffs, N.J., 1979.
(60) Gao, B.; Todd Walter, M.; Steenhuis, T. S.; Hogarth, W. L.; Parlange, J. Y. Rainfall induced chemical transport from soil to runoff: Theory and experiments. *J. Hydrol* **2004**, *295*, 291.
(61) Kim, Y.; Darnault, C. J. G.; Bailey, N. O.; Parlange, J.; Steenhuis, T. S. Equation for describing solute transport in field soils with preferential flow paths. *Soil Sci. Soc. Am. J.* **2005**, *69*, 291−300.
(62) Jacobsen, O. H.; Moldrup, P.; Larsen, C.; Konnerup, L.; Petersen, L. W. Particle transport in macropores of undisturbed soil columns. *J. Hydrol.* **1997**, *196*, 185−203.
(63) Shaw, S. B.; Walter, M. T.; Steenhuis, T. S. A physical model of particulate wash-off from rough impervious surfaces. *J. Hydrol.* **2006**, *327*, 618−626.
(64) Shaw, S. B.; Makhlouf, R.; Walter, M. T.; Parlange, J. Y. Experimental testing of a stochastic sediment transport model. *J. Hydrol.* **2008**, *348*, 425−430.
(65) Shaw, S. B.; Parlange, J. Y.; Lebowitz, M.; Walter, M. T. Accounting for surface roughness in a physically-based urban wash-off model. *J. Hydrol.* **2009**, *367*, 79−85.
(66) Wang, P.; Keller, A. A. Natural and engineered nano and colloidal transport: Role of zeta potential in prediction of particle deposition. *Langmuir* **2009**, *25*, 6856−6862.
(67) Li, Y.; Cu, Y. T.; Luo, D. Multiplexed detection of pathogen DNA with DNA-based fluorescence nanobarcodes. *Nat. Biotechnol.* **2005**, *23*, 885−889.
(68) Um, S. H.; Lee, J. B.; Kwon, S. Y.; Li, Y.; Luo, D. Dendrimer-like DNA-based fluorescence nanobarcodes. *Nat. Protoc.* **2006**, *1*, 995−1000.